

Article

Lithium Salt Catalyzed Ring-Opening Polymerized Solid-State Electrolyte with Comparable Ionic Conductivity and Better Interface Compatibility for Li-Ion Batteries

Wei Zhang ¹, Sujin Yoon ¹, Lei Jin ¹, Hyunmin Lim ¹, Minhyuk Jeon ¹, Hohyoun Jang ¹, Faiz Ahmed ² and Whangi Kim ^{1,*}

¹ Department of Applied Chemistry, Konkuk University, Chungju 27478, Korea; arno_zw@hotmail.com (W.Z.); ysj920126@naver.com (S.Y.); jinlei8761@naver.com (L.J.); tree3367@naver.com (H.L.); jeonminh97@naver.com (M.J.); 201417450@kku.ac.kr (H.J.)

² Grenoble INP, LEPMI, University of Grenoble Alpes, 38000 Grenoble, France; faiz2310@gmail.com

* Correspondence: wgkim@kku.ac.kr

Abstract: Rechargeable lithium-ion batteries have drawn extensive attention owing to increasing demands in applications from portable electronic devices to energy storage systems. In situ polymerization is considered one of the most promising approaches for enabling interfacial issues and improving compatibility between electrolytes and electrodes in batteries. Herein, we observed in situ thermally induced electrolytes based on an oxetane group with LiFSI as an initiator, and investigated structural characteristics, physicochemical properties, contacting interface, and electrochemical performances of as-prepared SPEs with a variety of technologies, such as FTIR, ¹H-NMR, FE-SEM, EIS, LSV, and chronoamperometry. The as-prepared SPEs exhibited good thermal stability (stable up to 210 °C), lower activation energy, and high ionic conductivity (>0.1 mS/cm) at 30 °C. Specifically, SPE-2.5 displayed a comparable ionic conductivity (1.3 mS/cm at 80 °C), better interfacial compatibility, and a high Li-ion transference number. The SPE-2.5 electrolyte had comparable coulombic efficiency with a half-cell configuration at 0.1 C for 50 cycles. Obtained results could provide the possibility of high ionic conductivity and good compatibility through in situ polymerization for the development of Li-ion batteries.

Keywords: in situ polymerization; interfacial issues; LiFSI; ionic conductivity; Li-ion battery



Citation: Zhang, W.; Yoon, S.; Jin, L.; Lim, H.; Jeon, M.; Jang, H.; Ahmed, F.; Kim, W. Lithium Salt Catalyzed Ring-Opening Polymerized Solid-State Electrolyte with Comparable Ionic Conductivity and Better Interface Compatibility for Li-Ion Batteries. *Membranes* **2022**, *12*, 330. <https://doi.org/10.3390/membranes12030330>

Academic Editor: Giovanni Battista Appetecchi

Received: 9 February 2022

Accepted: 10 March 2022

Published: 16 March 2022

Publisher's Note: MDPI stays neutral with regard to jurisdictional claims in published maps and institutional affiliations.



Copyright: © 2022 by the authors. Licensee MDPI, Basel, Switzerland. This article is an open access article distributed under the terms and conditions of the Creative Commons Attribution (CC BY) license (<https://creativecommons.org/licenses/by/4.0/>).

1. Introduction

Rechargeable Li-ion batteries (LiBs) have acted as an essential part of our daily lives in electronic items ranging from portable consumer electronic devices to large-scale transport equipment such as electric vehicles [1]. To date, conventional organic or inorganic liquid electrolytes (LEs) have some intrinsic or extrinsic properties (e.g., flammability, cost-inefficiency, and low ionic conductivity) that hinder extensive applications of current LiBs in energy storage and conversion systems. Extensive concern has been expressed about GPEs and SPEs due to their safety, thermal stability, and high voltage window [2]. Nevertheless, SPEs that can outperform LEs remain a challenge because of interfacial issues and compatibility between solid electrolytes and electrodes [3–5], which hinder Li⁺ transportation and impair the cycling performance of batteries. Thus, several strategies have been studied (e.g., thermally induced, free-radical, ionic, and ultraviolet (UV) in situ polymerization) for polymer electrolytes [6]. UV and thermally induced free-radical polymerization techniques still require development before they can be applied in industry.

In situ thermally induced CROP is considered one of the most promising approaches, with the advantages of effectively reducing interface resistance and enabling the compatibility of commercial components of LiBs production [2,3], which can produce the expected polymers for the development of SPEs. Several industrial polymers have been produced

through the CROP technique, such as polytetrahydrofurans, polysiloxanes, polyoxymethylene, and polyethyleneimines [7]. The CROP reaction can be initiated by Brønsted acids (e.g., HCl, H₂SO₄, HClO₄, and HOSO₂CF₃) and Lewis acids with co-initiators, photoinitiators, and onium ions [8]. BF₃ is one of the widely employed Lewis acids for CROP [2,3], as is its precursor boron trifluoride diethyl ether complex (BF₃ OEt₂) [9]. Moreover, common lithium salts such as lithium tetrafluoroborate (LiBF₄) [10], lithium perchlorate (LiClO₄) [2,9], lithium hexafluorophosphate (LiPF₆) [10], lithium difluoro(oxalato)borate (LiDFOB) [11], and lithium bis(trifluoromethane)sulfonimide (LiTFSI) [12] have been introduced into ring-opening polymerization because of their superacid anions. Lithium salts can also act as Lewis acids to activate the ring-opening polymerization reaction owing to their lower melting point and better solubility in low dielectric media [13]. For example, LiBF₄ can be treated like fluorine compounds and the Lewis acid BF₃, which has also been regarded as a superacid anion. Notably, aluminum triflate Al(CF₃SO₃)₃ and Al(OTf)₃ salts are efficient initiators for the polymerization of DOL [14]. The produced SPEs exhibit high ionic conductivity at ambient temperature, low interfacial resistance, highly coulombic efficiency (>99%), and long lifespan through in situ-formed SPEs. Some researchers have also studied polymerization based on the oxetane group using lithium salts as initiators, including LiBF₄ [15], LiPF₆ [10], and LiN(C₂F₅SO₂)₂ [9] with solvents. However, the poor conductivity of the obtained SPEs could be attributed to the incorporation of plasticizer or organic solvent (e.g., acetone, THF, acetonitrile) with inert fragility [2,13]. No additional solvents which take part in polymerized electrolytes are proposed. Compared with commercial LiPF₆, LiFSI has been extensively studied as a promising alternative conducting salt for LiBs, which not only exhibit superior stability and higher σ [16], but can also enhance electrochemical cyclability with graphite or Li metal anode [17,18]. Our group successfully fabricated siloxane-epoxy polymerized electrolytes (SEPEs) through in situ cationic ring opening, which illustrated low interfacial resistance, high conductivity (0.116 mS/cm), and a lithium transference number (t_{Li^+}) of 0.61 at room temperature. Moreover, the SEPEs also demonstrate a wide electrochemical stability window (up to ca. 4.7 V vs. Li/Li⁺) [19]. However, synthesized SEPEs with organic solvent could reduce battery safety [20]. Researchers have also studied polymer electrolytes with a trimethylene oxide (TMO) structure through the ring-opening polymerization of oxetane derivatives via lithium salts as an initiator [15,21]. However, the potential flammability and low ionic conductivity of poly(oxetane)-based electrolytes remain challenges in the application of lithium batteries.

Herein, we present a polymer electrolyte based on the oxetane-ring group, utilizing LiFSI salts as an initiator through in situ thermally induced CROP. LiFSI acted as H⁺ capturer, which was utilized to directly self-catalyze the CROP of EOM with an oxetane ring and a hydroxy group, in the absence of organic solvents. The prepared SPEs exhibited good thermostability, better interfacial compatibility among components in the cell, and comparable conductivity (>0.1 mS/cm). We hope this work provides a simplified and efficient assembly strategy for the development of solid-state LiBs.

2. Experimental

2.1. Chemicals

EOM (96%) was purchased from TCI company (Tokyo, Japan). LiFePO₄ (LFP)-coated Al foil and lithium foil were obtained from MTI corporation (Richmond, CA, USA). High-purity LiFSI (99.9%), DMSO-*d*₆, LiCoO₂ (LCO), poly(vinylidene difluoride) (PVDF), and carbon black (CB) were obtained from Sigma Aldrich (St. Louis, MO, USA), and were used as received unless stated otherwise. Besides, there is a list of abbreviation nomenclature for this article in Table S1.

2.2. Instruments and Measurements

The structural characteristics of as-synthesized electrolytes were analyzed by FTIR spectra (Nicolet iS5, ASB1100426, Thermo Fisher Scientific, Waltham, MA, USA) and ¹H-

NMR (Avance 400FT-NMR (400 Hz), Bruker DRX, Seongnam Korea) with tetramethyl silane (TMS) as a reference. DMSO- d_6 was used as a solvent. Thermal properties were recorded with a Scinco TGA-N 1000 (Seoul, Korea) analyzer from 30 °C to 600 °C at a heating rate of 10 °C/min in the presence of N₂ atmosphere. The viscosities of electrolytes were observed with a viscometer (*lts*-VROCTM, RheoSense, San Ramon, CA, USA). The morphology of the electrolytes and electrodes inside the cell was attained with a field-emission scanning electron microscope (FE-SEM, JEOL 7401 F, JEOL, Tokyo, Japan).

2.3. Fabrication of Asymmetry Dummy Cell

An asymmetric dummy cell was assembled for evaluating the conductivity of the as-synthesized electrolytes, and its configuration is shown in Figure 1. Typically, for cathode electrodes, the composition of slurry paste was LCO (86 wt%), CB (5 wt%), and PVDF (9 wt%). The LiCoO₂-coated electrode was prepared by doctor-blading a home-made paste on a clean FTO glass electrode (active area: ca. 0.138 cm²; thickness: ca. 10 μm) and dried at 80 °C overnight in a vacuum oven. Similarly, a graphite anode electrode was also fabricated on a cleaned FTO glass electrode (active area: ca. 0.138 cm²; thickness: ca. 12 μm) using a homemade paste consisting of carbon black and PVDF of 90 and 10 wt%, respectively.

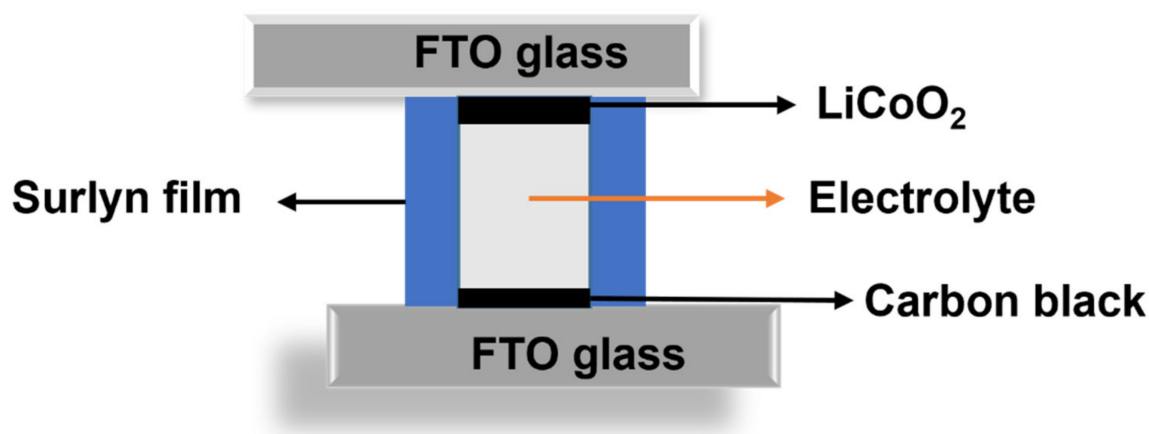


Figure 1. Schematic diagram of an asymmetric dummy cell.

2.4. In Situ Thermal Polymerization

Cationic ring-opening polymerization of EOM was initiated directly with LiFSI salt. The precursor EOM (1 mL, 8.78 mmol) and LiFSI salt (376 mg, 2.01 mmol) were mixed in 5 mL bottle under a N₂-filled glove box and the solution was stirred for 2 h to make a homogeneous solution. Afterward, the homogeneous liquid solution was placed in an environment with a constant temperature of 60 °C for 48 h. To evaluate ionic conductivity, freshly prepared homogeneous liquid solution was injected into the dummy cell through the pre-drilled hole on the FTO glass electrode, sealed using Scotch tape, and kept in the same environment. The as-prepared electrolyte of 2 M LiFSI in EOM was designated as SPE-2. Similarly, the electrolytes of 2.5 M LiFSI and 3 M LiFSI in EOM were denoted as SPE-2.5 and SPE-3, respectively.

2.5. Electrochemical Performances

All the EIS analysis was conducted with an IM6ex (Zahner-Elektrik GmbH & Co. KG instrument, Kronach, Germany) for measuring the ionic conductivity (σ) of as-prepared electrolytes in the temperature range from 30 to 80 °C at an interval of 10 °C, within the frequency range of 0.1 Hz to 10⁵ Hz at the open-circuit potential, and with an AC amplitude of 5 mV. The cells were allowed to reach thermal equilibrium for 40 min before each test. Then, the data of EIS spectra were fitted with an equivalent circuit model using Z-view

software (version 3.1, Scribner Associates Inc., Southern Pines, NC, USA). The value of σ was calculated according to the following equation.

$$\sigma = \frac{l}{AR} \quad (1)$$

where σ is the ionic conductivity, l is the distance between the two electrodes, R is the bulk resistance, and A is the active area of the electrode surface in contact with electrolytes.

The electrochemical measurements of as-prepared SPEs were assembled inside the glovebox under Ar-filled environment (H_2O and $\text{O}_2 < 0.1$ ppm) and carried out on an Ivium-n-Stat (Ivium Technologies, Eindhoven, The Netherlands). The electrochemical stability of SPEs was studied using LSV technology. All of the electrolytes were assembled based on Li/SPEs/LFP cells at room temperature and a constant rate of 1.0 mV/s from 0 V to 5 V. The t_{Li^+} was also observed by the Swagelok cell (Figure S1). Then, the t_{Li^+} of SPEs was calculated from the Bruce–Vincent–Evans Equation (2) [22,23].

$$t_{\text{Li}^+} = (I_s(\Delta U - I_0 R_0)) / (I_0(\Delta U - I_s R_s)) \quad (2)$$

where I_0 , I_s , R_0 , R_s , and ΔU are initial current, steady-state current, interfacial resistance without and with polarization, and applied DC polarization voltage, respectively.

3. Results and Discussion

3.1. Chemical Structure Characterization

The fact that the color of electrolytes was untransparent and unstable (Figure S2) with low concentrations (1 M and 1.5 M) of LiFSI meant that the in situ polymerization was not successful; therefore, we selected SPE-2.5 to evaluate the polymerization condition.

The chemical structure of SPE-2.5 was confirmed by $^1\text{H-NMR}$ and FTIR spectroscopy (as Figure 2a,c shows, respectively). The detailed $^1\text{H-NMR}$ analytical data are listed as follows. $^1\text{H-NMR}$ ($\text{DMSO-}d_6$, ppm): $\delta = 0.81$ (t, 3H), 1.26 (s, 2H), 1.61 (q, 2H), 3.15 (s, 2H), 3.26 (m, 2H), 3.5 (d, 2H), 4.2 (dd, 2H), 4.3 (dd, 2H), and 4.8 (t, 1H). The number-average molecular weight of poly (EOM) was estimated from the relative intensities of the NMR peaks between the terminal structure (3.5 ppm) and the main chains (3.24 ppm), which was 7640 [15]. However, the estimated molecular weights of SPE-2 and SPE-3 were ca. 4920 and ca. 6090, respectively, estimated from their NMR spectra (Figure S3a,b). Poly (EOM)-based SPEs have two possible sites which coordinate with lithium ions. One is the terminal hydroxy group, which probably possesses the good solubility of Li salts; the other one is the trimethylene oxide moiety in the backbone [15].

Figure 2b exhibits the FTIR spectra of SPEs. For comparison, we also measured the FTIR spectra of the precursor EOM. As-prepared SPEs displayed the disappearance or reduction of the peak at ca. 960 cm^{-1} (Figure 2b,c), which can be attributed to the functional group -C-O-C [24] indicating the successful polymerization of poly (EOM). The broad peaks in the range of $3100\text{--}3700\text{ cm}^{-1}$ for all electrolytes indicate the presence of H-bonded N anions along with the trace amounts of physisorbed water molecules [25]. SPEs also displayed the main peaks of $-\text{CH}_3$ and $-\text{CH}_2$ stretching at 2962 and 2882 cm^{-1} , respectively. In addition, the peak at 840 cm^{-1} is ascribed to Li-O rocking, indicating the interaction of ether oxygen atoms with Li ion [24].

To further confirm polymerization, we investigated the conversion rate (CR) of the polymerized electrolyte, which was evaluated by measuring the peak area of oxetane ether bands (ca. 960 cm^{-1} or 840 cm^{-1}) at each time point of the reaction, and determined using the following Equation (3) [10,26]:

$$\text{Conversion rate} = \frac{A_0 - A_t}{A_0} \times 100\% \quad (3)$$

where CR is the conversion at time t , and A_0 and A_t are the peak areas of the functional groups before polymerization and at time t , respectively. Figure 3 shows the polymerization

CR of synthesized SPEs, and the CR values of SPE-2, SPE-2.5, and SPE-3 reached ca. 60.52%, 65.42% and 72.46%, respectively. These results indicate the presence of SPEs, along with unreacted start materials, and that the suitable mole ratio of Li to O played a vital role in the polymerization process [27].

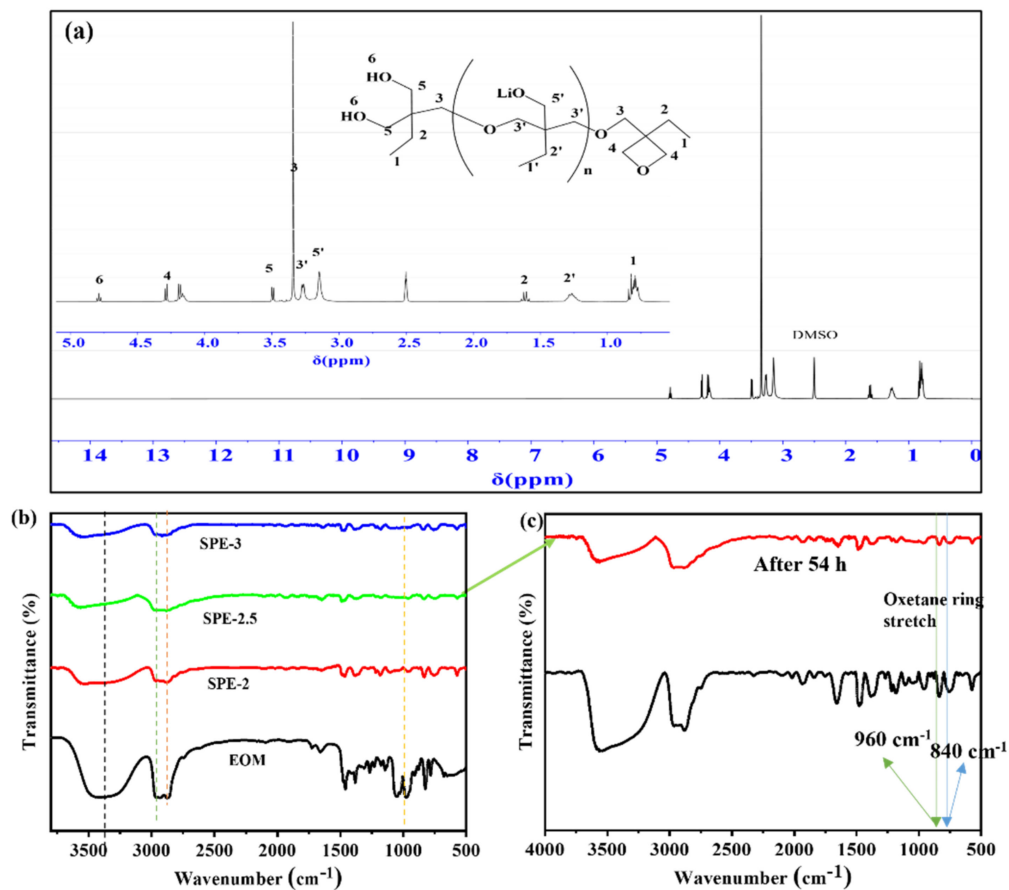


Figure 2. (a) $^1\text{H-NMR}$ spectra (inset shows the partial enlarged $^1\text{H-NMR}$ spectra) of SPE-2.5, (b) FTIR spectra of precursor EOM and SPEs and (c) initial transmittance and after 54 h of SPE-2.5.

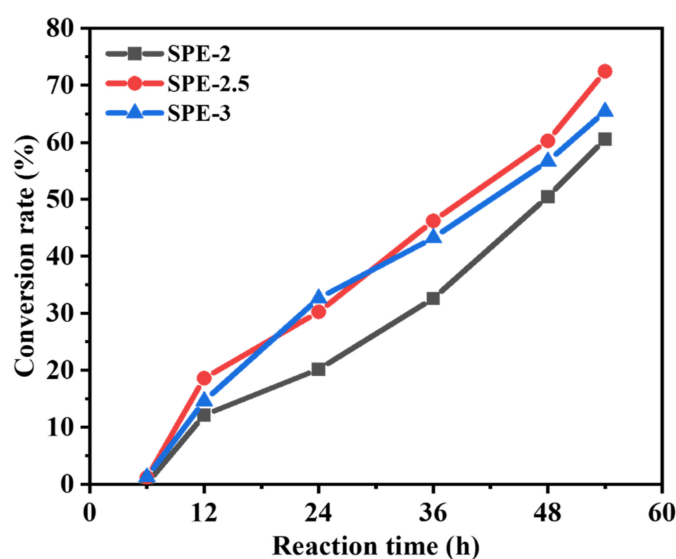


Figure 3. Conversion rate vs. reaction time plots of SPE-2, SPE-2.5, and SPE-3.

3.2. Physicochemical Properties of SPEs

Figure 4a shows the TGA plots of SPE-2, SPE-2.5, and SPE-3. All the SPEs exhibited a two-step weight loss. The weight loss (ca. 12%) up to 210 °C in the first step can be ascribed to the loss of physisorbed water molecules and the incorporation of LiFSI, which is consistent with the reported work [25,28]. Then, all SPEs experienced a sharp weight loss up to 500 °C, and the weight losses of SPE-3, SPE-2.5, and SPE-2 were ca. 75%, 78%, and 82%, respectively. The residual weights (%) of SPE-2, SPE-2.5, and SPE-3 were ca. 9%, 14%, and 24%, respectively, up to 600 °C. This is probably ascribable to residual carbon compounds from their decomposition, which needs further in-depth observation. The residual percentage of SPE-3 was higher than those of SPE-2 and SPE-2.5 because of the high concentration of lithium salt.

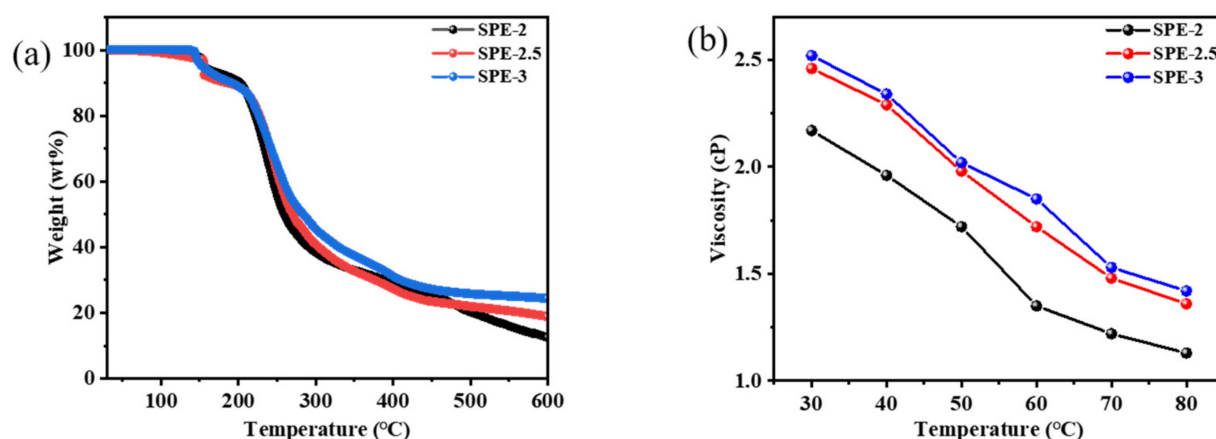


Figure 4. TGA traces (a) and viscosity vs. temperature curves (b) of SPE-2, SPE-2.5, and SPE-3.

Figure 4b exhibits the viscosities of SPE-2 (1 M), SPE-2.5 (1 M), and SPE-3 (1 M) which were evaluated by dissolving them in DMSO. Their viscosities were ca. 2.17, ca. 2.46, and ca. 2.52 cP at 30 °C, respectively. Nevertheless, at 80 °C, their dynamic viscosities decreased to ca. 1.13, ca. 1.36, and ca. 1.42 cP, respectively. As the temperature increased, the dynamic viscosity of the electrolyte presented a decreasing trend, which can be ascribed to the weakening intermolecular forces in the electrolyte [25]. This low viscosity of all SPEs implies that they possess the capacity of conducting lithium ions with high conductivity.

3.3. Electrochemical Performances

3.3.1. Ionic Conductivity and Impedimetric Stability

The conductivity was evaluated using EIS technology, and the σ values of SPE-2, SPE-2.5, and SPE-3 were calculated from Nyquist plots, fitting results with an equivalent circuit (Figure S4); the calculated values were 0.14 mS/cm, 0.25 mS/cm, and 0.16 mS/cm at 30 °C, respectively. The conductivities of SPE-2, SPE-2.5, and SPE-3 were 0.88 mS/cm, 1.3 mS/cm, and 1.1 mS/cm at 80 °C, respectively. These conductivity values were higher than reported poly (oxetane)-based electrolytes [9,10]. Moreover, the conductivity of SPE-2.5 was higher than those of SPE-2 and SPE-3, which indicated a suitable concentration of Li salt enhanced the conductivity of the electrolyte [10,23]. To study the temperature dependence σ of as-synthesized SPEs, we drew $\ln \sigma$ vs. the inverse of absolute temperatures, as displayed in Figure 5b. The plot indicates a linear dependency of $\ln \sigma$ along with temperature, which agrees with the typical Arrhenius plot. The activation energy (E_a) was calculated from Arrhenius plots. The E_a of SPE-2.5 (ca. 0.25 eV) was lower than those of SPE-2 and SPE-3, which were ca. 0.3 eV and ca. 0.32 eV, respectively. The low E_a of electrolytes could be ascribed to the weak binding energies between the Li^+ cation and the corresponding anions, and facilitates high ionic conductivity [29,30].

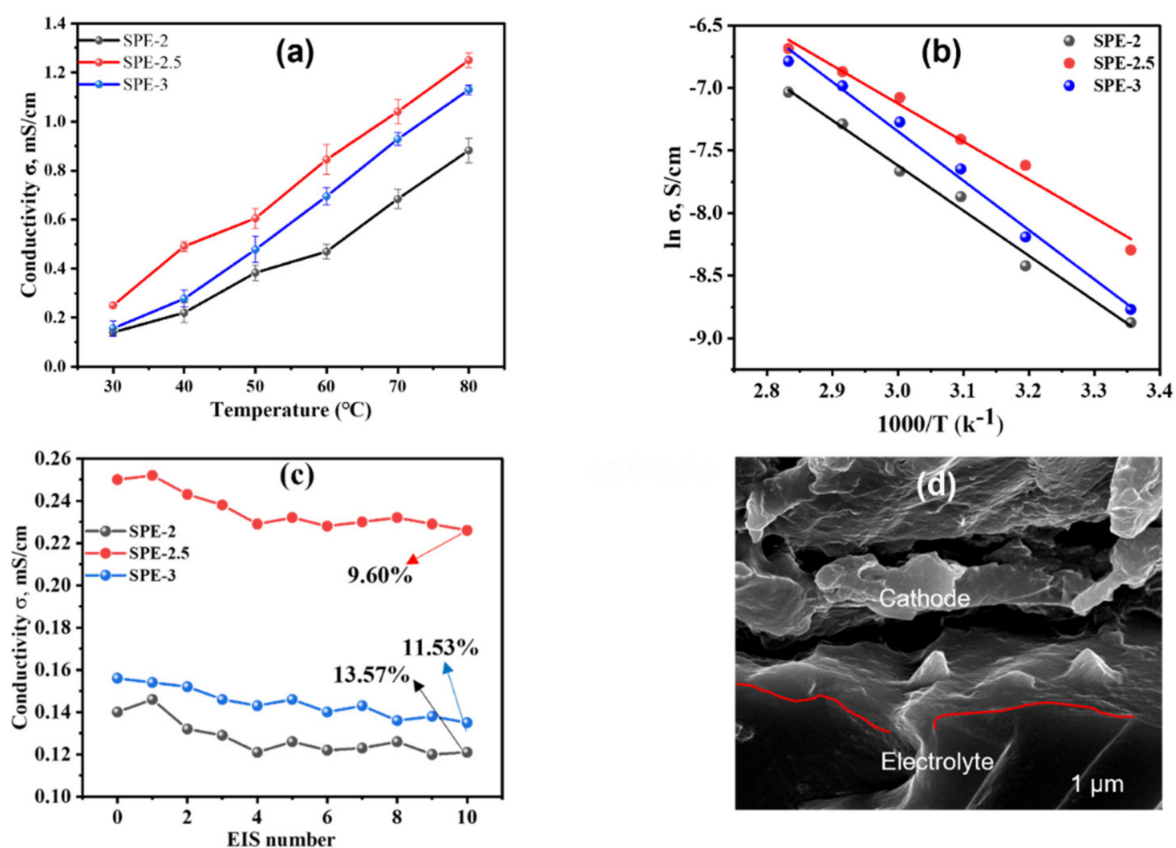


Figure 5. Plots of conductivity vs. temperature (a) and $\ln(\text{Li}^+$ conductivity) vs. the inverse of absolute temperature (b) of SPEs. (c) Variation of the conductivity of SPEs with repetitive EIS scanning for SPE-2, SPE-2.5, and SPE-3, at 25 $^{\circ}\text{C}$ and open circuit condition. (d) Cross-sectional FE-SEM image after 50 cycles from dummy cell of SPE-2.5.

The successive EIS measurements were utilized to investigate the electrochemical stability of SPE-2, SPE-2.5, and SPE-3. The series of EIS measurements were as follows: 10 CV sweeps (potential range from -1.5 to 5 V, scan rate 25 mV/s); relaxation at 0 V (1 min). This series of electrochemical stability testing was repeated 11 times. Figure 5c displays the change of σ values along with the number of EIS scans. The σ values of all electrolytes were decreased after CV sweeping, and were ca. 22.85%, ca. 9.60%, 19.23% for SPE-2, SPE-2.5, and SPE-3, respectively. This indicates that these SPEs may develop the electrochemical stability of LiBs. Additionally, the FE-SEM image (Figure 5d) of SPE-2.5 displays good electrolyte/electrode contact, which also facilitates conductivity. Meanwhile, the SEM image also reveals that good compatibility of electrolytes and electrodes could enhance electrochemical stability (Figure S5) [19].

3.3.2. Electrochemical Stability Window and t_{Li^+} Measurement

Figure 6a displays the kinetic ESW of as-prepared SPEs. The oxidation potentials (vs. Li/Li^+) of SPE-2, SPE-2.5, and SPE-3 were up to ca. 3.0, 3.75, and 3.4 V, respectively. Notably, the working potential of SPE-2.5 was a little higher than those of LiFePO_4 (3.4 V), $\text{LiNi}_{1/3}\text{Mn}_{1/3}\text{Co}_{1/3}\text{O}_2$ (NMC) (3.7 V), $\text{LiNi}_{0.8}\text{Co}_{0.15}\text{Al}_{0.05}\text{O}_2$ (NCA) (3.7 V), and $0.5\text{Li}_2\text{MnO}_3 \cdot 0.5\text{LiMO}_2$ (3.6 V), which are current commercially available cathodes [31]. The low operation potentials of SPE-2 and SPE-3 were due to the abundant hydroxy group coactions and the weak motion of lithium ions in the electrolyte.

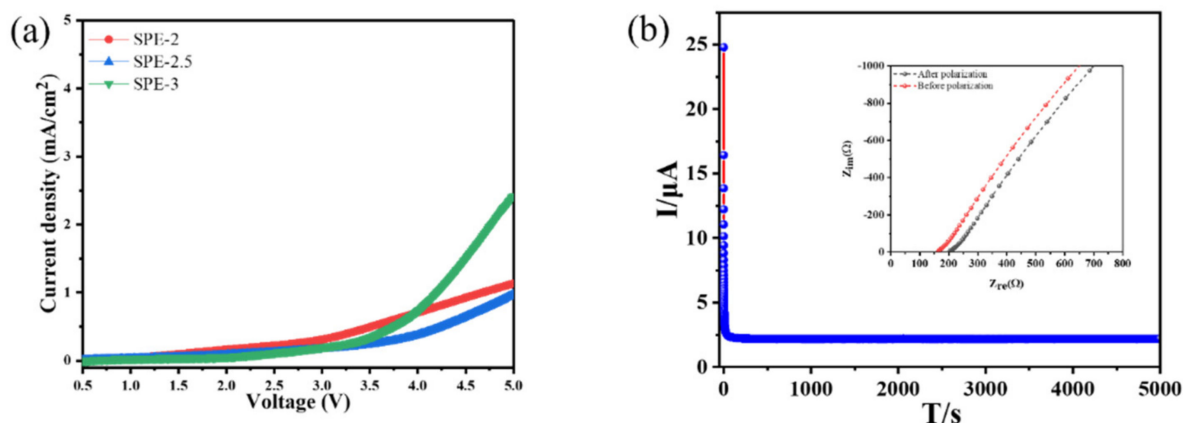


Figure 6. (a) Current density vs. voltage plot of SPE-2, SPE-2.5, and SPE-3. (b) Chronoamperometric polarization plot of the electrolyte-based symmetry Li/SPE-2.5/Li Swagelok cell at 10 mV for 5000 s (inset exhibits the Nyquist curves of the cell before and after polarization).

The t_{Li^+} of the electrolyte plays an important role in evaluating the electrochemical performance of LiBs. Based on the values of σ and ESW, we only studied the t_{Li^+} of SPE-2.5. The homogeneous liquid electrolyte was injected into a Teflon chamber and sealed in a Swagelok cell in an Ar-filled environment glovebox and kept at 60 °C for 54 h. After complete polymerization, the cell was cooled to ambient temperature. Measurements were carried out at 25 °C. Figure 6b displays the chronoamperometric traces of the symmetrical Swagelok cell at the applied voltage of 10 mV and the inset of Figure 6b exhibits the Nyquist plots of the cell before and after polarization. The details of the analytical parameters of chronoamperometric and Nyquist Plots are summarized in Table S2, which obtained the t_{Li^+} of ca. 0.74. The t_{Li^+} of this electrolyte was much higher than what has been reported in the literature, as summarized in Table S3. This indicates that Li⁺ is mainly carried for ionic charge in the SPE-2.5, rather than the counter anion [25].

3.3.3. Electrochemical Performances

In general, higher ionic conductivity of electrolytes correlates well with better electrochemical performance. Thus, we investigated the battery performance of SPE-2.5 with a device configuration of LiFePO₄/SPE-2.5/Li metal. Due to stable cycling performance, high theoretical capacity (170 mAh/g at 0.1 C), and a high tolerance to overcharge [22,25], LiFePO₄ was used as a cathode material. The C-rate was calculated by cathode material weight (12.80 mg/cm²).

Figure 7a demonstrates the CD profiles of LiFePO₄/SPE-2.5/Li at 1st, 25th, and 50th cycle numbers over the potential range of 2.5–4.2 V at 0.1 C. The discharge specific capacities of SPE-2.5 containing the half-cell after 1st, 25th, and 50th cycles were ca. 141, 129, and 120 mAh/g, respectively. At the same time, the corresponding charge specific capacities of this electrolyte were ca. 157, 137, and 125 mAh/g, respectively. Figure 7b exhibits the variation of C_{sp} and η with the number of CD cycles at 0.1 C. The C_{sp} of SPE-2.5 electrolyte-based half-cell was ca. 120 mAh/g at 0.1 C after 50 CD cycles, which retained 85.11% of initial C_{sp} . This could be ascribed to the effect of LiFePO₄ cathode material thickness (our LiFePO₄ thickness was ca. 55 μm) during the in situ polymerization process [32]. In addition, the η of the half-cell was ca. 95.25% after 50 CD cycles, indicating that there was a highly reversible positive electrochemical reaction. Over 2 M LiFSI in electrolytes probably generates solid electrolyte layers, which facilitate cycling performances of Li metal anode [33]. Thereof, these results suggest that SPE-2.5 electrolyte is promising for the development of Li-ion batteries.

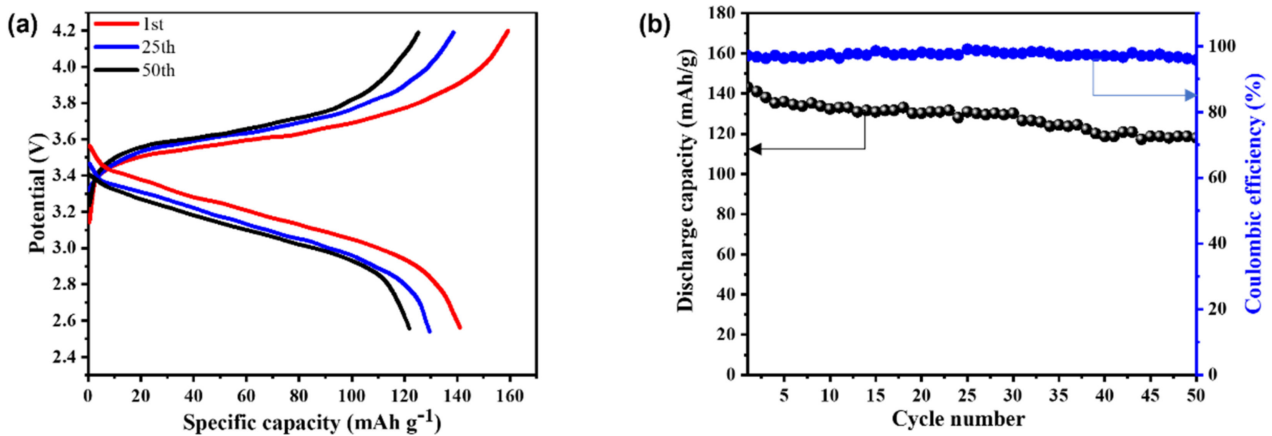


Figure 7. CD plots of SPE-2.5 with structure of LiFePO₄/SPE-2.5/Li cell for 0.1 C over a potential range of 2.5–4.2 V at 25 °C (a), discharge capacity and coulombic efficiency of CD cycling number of the LiFePO₄/SPE-2.5/Li cell at 0.1 C and 25 °C (b).

3.3.4. Mechanism of In Situ Cationic Ring Opening of Poly (EOM)

According to our experimental results, a plausible self-catalyzed cationic ring-opening polymerization mechanism (Figure 8a) and merits of in situ polymerization (Figure 8b) were presented. Due to the absence of an inflammable solvent, as-prepared SPEs could improve the safety performance of batteries. Ionic conductivity was observed to be better in SPE-2.5 than in SPE-2 and SPE-3, suggesting that abundant OH groups and highly concentrated Li salt affected the Li⁺ ion mobility in poly (EOM). Additionally, SPE-2.5 demonstrated a comparable C_{sp} and η, which could be applied in Li-ion batteries.

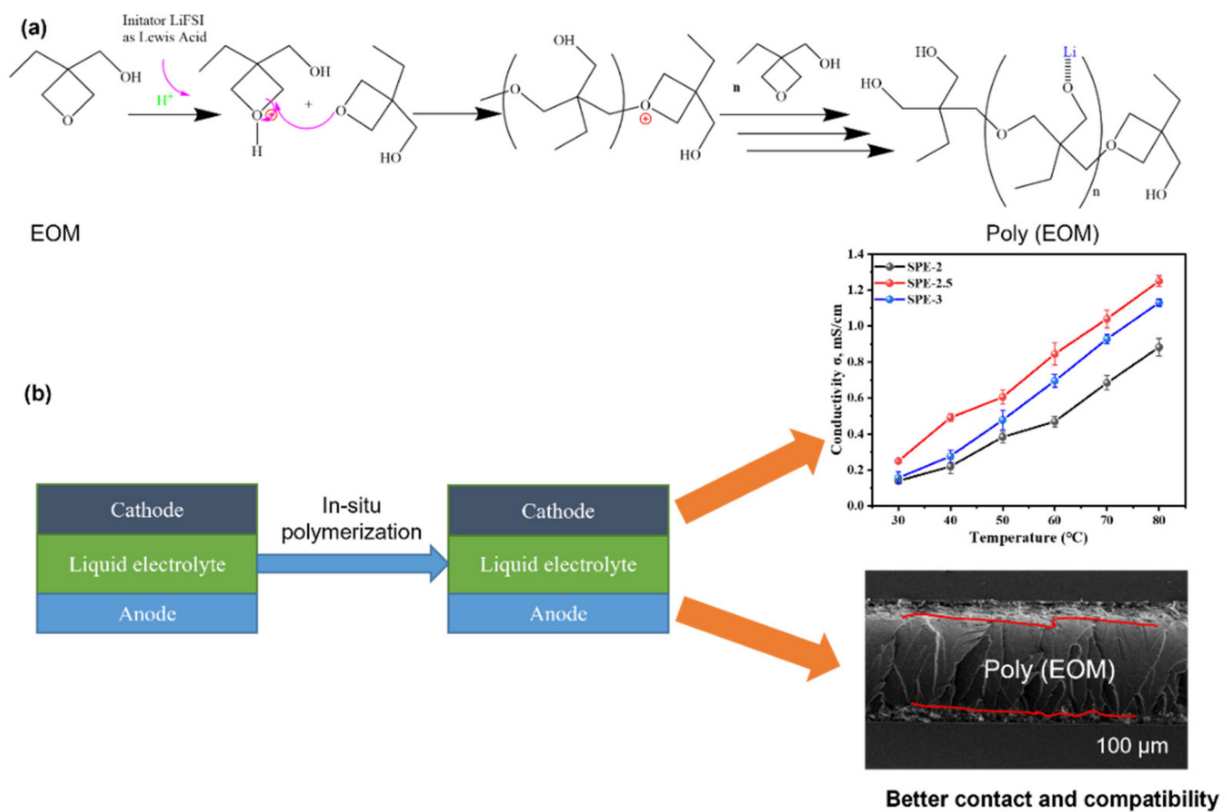


Figure 8. (a) Schematic illustration of cationic ring-opening polymerization of poly (EOM), (b) advantages of in situ polymerization.

4. Conclusions

Herein, we successfully synthesized a solid polymer electrolyte based on poly (EOM) via an in situ polymerization strategy with LiFSI as an initiator. The in situ polymerization approach greatly simplified the fabrication process of polymer electrolytes for LiBs. Furthermore, the in situ-constructed framework of SPEs remarkably enhanced the contact compatibility and interfacial stability between the SPEs and the electrodes. Additionally, we obtained SPEs which exhibited considerable conductivity owing to the absence of organic solvent and the compatibility of LiFSI with anode. The as-prepared SPE-2.5 possessed comparable conductivity (0.25 mS/cm at 30 °C and 1.3 mS/cm at 80 °C), oxidation stability up to 3.75 V, high t_{Li^+} (0.74), and cycling performance after 50 charge–discharge cycles. These results suggest a strategy which favors the consideration of the in situ-formed poly (EOM)-based polymer electrolyte as a promising candidate for lithium-metal rechargeable batteries.

Supplementary Materials: The following supporting information can be downloaded at: <https://www.mdpi.com/article/10.3390/membranes12030330/s1>, Figure S1: Configuration of symmetry Swagelok cell; Figure S2: Photographing of varied concentrated LiFSI with EOM after 54 h; Figure S3: $^1\text{H-NMR}$ spectrum of SPE-3 (a) and SPE-2 (b); Figure S4: Nyquist curves of SPE-2 (a), SPE-2.5 with corresponding fitting plots (b) and SPE-3 (c); equivalent circuit (d); Figure S5: CV sweeping 50 cycles of SPE-2.5 electrolyte with the dummy cell over the potential range from -1.5 to 5 V, scan rate at 25 mV/s; Table S1: The explanation of abbreviation words used in this article; Table S2: Analytical parameters for the calculation of t_{Li^+} of SPE-2.5; Table S3: Comparison of properties of polymer electrolyte reported based on ring-opening polymerization. References [34–38] have been cited in Supplementary Materials.

Author Contributions: Writing—original draft, W.Z.; validation, S.Y.; formal analysis, L.J.; resources, H.L.; software, M.J.; writing—review and editing, F.A.; supervision, H.J.; project administration, W.K. All authors have read and agreed to the published version of the manuscript.

Funding: This research received no external funding.

Institutional Review Board Statement: Not Applicable.

Informed Consent Statement: Not Applicable.

Data Availability Statement: The data presented in this study are available on request from the corresponding author.

Acknowledgments: This work was supported by Konkuk University 2021.

Conflicts of Interest: The authors declare no conflict of interest.

References

1. Liu, K.; Liu, Y.; Lin, D.; Pei, A.; Cui, Y. Materials for lithium-ion battery safety. *Sci. Adv.* **2018**, *4*, aas9820. [[CrossRef](#)] [[PubMed](#)]
2. Huang, S.; Cui, Z.; Qiao, L.; Xu, G.; Zhang, J.; Tang, K.; Liu, X.; Wang, Q.; Zhou, X.; Zhang, B.; et al. An in-situ polymerized solid polymer electrolyte enables excellent interfacial compatibility in lithium batteries. *Electrochim. Acta* **2019**, *299*, 820–827. [[CrossRef](#)]
3. Cui, Y.; Liang, X.; Chai, J.; Cui, Z.; Wang, Q.; He, W.; Liu, X.; Liu, Z.; Cui, G.; Feng, J. High Performance Solid Polymer Electrolytes for Rechargeable Batteries: A Self-Catalyzed Strategy toward Facile Synthesis. *Adv. Sci.* **2017**, *4*, 1700174. [[CrossRef](#)] [[PubMed](#)]
4. Ding, P.; Lin, Z.; Guo, X.; Wu, L.; Wang, Y.; Guo, H.; Li, L.; Yu, H. Polymer electrolytes and interfaces in solid-state lithium metal batteries. *Mater. Today* **2021**, *51*, 449–474. [[CrossRef](#)]
5. Geng, Z.; Huang, Y.; Sun, G.; Chen, R.; Cao, W.; Zheng, J.; Li, H. In-situ polymerized solid-state electrolytes with stable cycling for Li/LiCoO₂ batteries. *Nano Energy* **2022**, *91*, 106679. [[CrossRef](#)]
6. Vijayakumar, V.; Anothumakkool, B.; Kurungot, S.; Winter, M.; Nair, J.R. In situ polymerization process: An essential design tool for lithium polymer batteries. *Energy Environ. Sci.* **2021**, *14*, 2708–2788. [[CrossRef](#)]
7. Nuyken, O.; Pask, S. Ring-Opening Polymerization—An Introductory Review. *Polymers* **2013**, *5*, 361–403. [[CrossRef](#)]
8. Crivello, J.V. Investigations of the reactivity of “kick-started” oxetanes in photoinitiated cationic polymerization. *J. Polym. Sci. A Polym. Chem.* **2015**, *53*, 586–593. [[CrossRef](#)]
9. Shintani, Y.; Tsutsumi, H. Ionic conducting behavior of solvent-free polymer electrolytes prepared from oxetane derivative with nitrile group. *J. Power Sources* **2010**, *195*, 2863–2869. [[CrossRef](#)]

10. Miwa, Y.; Tsutsumi, H.; Oishi, T. New Type Polymer Electrolytes Based on Bis-Oxetane Monomer with Oligo(ethylene oxide) Units. *Polym. J.* **2001**, *33*, 927–933. [[CrossRef](#)]
11. Ma, Y.; Sun, Q.; Wang, S.; Zhou, Y.; Song, D.; Zhang, H.; Shi, X.; Zhang, L. Li salt initiated in-situ polymerized solid polymer electrolyte_new insights via in-situ electrochemical impedance spectroscopy. *Chem. Eng. J.* **2022**, *429*, 132483. [[CrossRef](#)]
12. Natarajan, A.; Stephan, A.M.; Chan, C.H.; Kalarikkal, N.; Thomas, S. Electrochemical studies on composite gel polymer electrolytes for lithium sulfur-batteries. *J. Appl. Polym. Sci.* **2017**, *134*, 44594–44601. [[CrossRef](#)]
13. Andrews, W.T.; Liebig, A.; Cook, J.; Marsh, P.; Ciocanel, C.; Lindberg, G.E.; Browder, C.C. Development of a PEO-based lithium ion conductive epoxy resin polymer electrolyte. *Solid State Ion.* **2018**, *326*, 150–158. [[CrossRef](#)]
14. Zhao, Q.; Liu, X.; Stalin, S.; Khan, K.; Archer, L.A. Solid-state polymer electrolytes with in-built fast interfacial transport for secondary lithium batteries. *Nat. Energy* **2019**, *4*, 365–373. [[CrossRef](#)]
15. Shibutani, R.; Tsutsumi, H. Fire-retardant solid polymer electrolyte films prepared from oxetane derivative with dimethyl phosphate ester group. *J. Power Sources* **2012**, *202*, 369–373. [[CrossRef](#)]
16. Han, H.-B.; Zhou, S.-S.; Zhang, D.-J.; Feng, S.-W.; Li, L.-F.; Liu, K.; Feng, W.-F.; Nie, J.; Li, H.; Huang, X.-J. Lithium bis(fluorosulfonyl)imide (LiFSI) as conducting salt for nonaqueous liquid electrolytes for lithium-ion batteries: Physicochemical and electrochemical properties. *J. Power Sources* **2011**, *196*, 3623–3632. [[CrossRef](#)]
17. Kang, S.-J.; Park, K.; Park, S.-H.; Lee, H. Unraveling the role of LiFSI electrolyte in the superior performance of graphite anodes for Li-ion batteries. *Electrochim. Acta* **2018**, *259*, 949–954. [[CrossRef](#)]
18. Shkrob, I.A.; Marin, T.W.; Zhu, Y.; Abraham, D.P. Why Bis(fluorosulfonyl)imide Is a “Magic Anion” for Electrochemistry. *J. Phys. Chem. C* **2014**, *118*, 19661–19671. [[CrossRef](#)]
19. Jin, L.; Jang, G.; Lim, H.; Zhang, W.; Kim, W.; Jang, H. An In Situ Polymeric Electrolyte with Low Interfacial Resistance on Electrodes for Lithium-Ion Batteries. *Adv. Mater. Interfaces* **2021**, *9*, 2101958. [[CrossRef](#)]
20. Liu, T.; Zhang, J.; Han, W.; Zhang, J.; Ding, G.; Dong, S.; Cui, G. Review—In Situ Polymerization for Integration and Interfacial Protection Towards Solid State Lithium Batteries. *J. Electrochem. Soc.* **2020**, *167*, 070527. [[CrossRef](#)]
21. Ye, L.; Feng, Z.-g.; Su, Y.-f.; Wu, F.; Chen, S.; Wang, G.-q. Synthesis and characterization of homo- and copolymers of 3-(2-cyano ethoxy)methyl- and 3-[methoxy(triethylenoxy)]methyl-3'-methyl-oxetane. *Polym. Int.* **2005**, *54*, 1440–1448. [[CrossRef](#)]
22. Ahmed, F.; Choi, I.; Rahman, M.M.; Jang, H.; Ryu, T.; Yoon, S.; Jin, L.; Jin, Y.; Kim, W. Remarkable Conductivity of a Self-Healing Single-Ion Conducting Polymer Electrolyte, Poly(ethylene-co-acrylic lithium (fluoro sulfonyl)imide), for All-Solid-State Li-Ion Batteries. *ACS Appl. Mater. Interfaces* **2019**, *11*, 34930–34938. [[CrossRef](#)] [[PubMed](#)]
23. Yao, W.; Zhang, Q.; Qi, F.; Zhang, J.; Liu, K.; Li, J.; Chen, W.; Du, Y.; Jin, Y.; Liang, Y.; et al. Epoxy containing solid polymer electrolyte for lithium ion battery. *Electrochim. Acta* **2019**, *318*, 302–313. [[CrossRef](#)]
24. Yang, Q.; Pan, X.; Huang, F.; Li, K. Synthesis and characterization of cellulose fibers grafted with hyperbranched poly(3-methyl-3-oxetanemethanol). *Cellulose* **2011**, *18*, 1611–1621. [[CrossRef](#)]
25. Ahmed, F.; Rahman, M.M.; Sutradhar, S.C.; Lopa, N.S.; Ryu, T.; Yoon, S.; Choi, I.; Lee, Y.; Kim, W. Synthesis and electrochemical performance of an imidazolium based Li salt as electrolyte with Li fluorinated sulfonylimides as additives for Li-Ion batteries. *Electrochim. Acta* **2019**, *302*, 161–168. [[CrossRef](#)]
26. Nair, J.R.; Shaji, I.; Ehteshami, N.; Thum, A.; Diddens, D.; Heuer, A.; Winter, M. Solid Polymer Electrolytes for Lithium Metal Battery via Thermally Induced Cationic Ring-Opening Polymerization (CROP) with an Insight into the Reaction Mechanism. *Chem. Mater.* **2019**, *31*, 3118–3133. [[CrossRef](#)]
27. Homann, G.; Stolz, L.; Nair, J.; Laskovic, I.C.; Winter, M.; Kasnatscheew, J. Poly(Ethylene Oxide)-based Electrolyte for Solid-State-Lithium-Batteries with High Voltage Positive Electrodes: Evaluating the Role of Electrolyte Oxidation in Rapid Cell Failure. *Sci. Rep.* **2020**, *10*, 4390. [[CrossRef](#)]
28. Kerner, M.; Plylahan, N.; Scheers, J.; Johansson, P. Thermal stability and decomposition of lithium bis(fluorosulfonyl)imide (LiFSI) salts. *RSC Adv.* **2016**, *6*, 23327–23334. [[CrossRef](#)]
29. Li, L.; Zhou, S.; Han, H.; Li, H.; Nie, J.; Armand, M.; Zhou, Z.; Huang, X. Transport and Electrochemical Properties and Spectral Features of Non-Aqueous Electrolytes Containing LiFSI in Linear Carbonate Solvents. *J. Electrochem. Soc.* **2011**, *158*, A74–A82. [[CrossRef](#)]
30. Kerr, J.B.; Liu, G.; Curtiss, L.A.; Redfern, P.C. Towards room-temperature performance for lithium–polymer batteries. *Electrochim. Acta* **2003**, *48*, 2305–2309. [[CrossRef](#)]
31. Croy, J.R.; Abouimrane, A.; Zhang, Z. Next-generation lithium-ion batteries: The promise of near-term advancements. *MRS Bull.* **2014**, *39*, 407–415. [[CrossRef](#)]
32. Jeong, J.; Lee, H.; Choi, J.; Ryou, M.-H.; Lee, Y.M. Effect of LiFePO₄ cathode density and thickness on electrochemical performance of lithium metal polymer batteries prepared by in situ thermal polymerization. *Electrochim. Acta* **2015**, *154*, 149–156. [[CrossRef](#)]
33. Wang, M.; Huai, L.; Hu, G.; Yang, S.; Ren, F.; Wang, S.; Zhang, Z.; Chen, Z.; Peng, Z.; Shen, C. Effect of LiFSI Concentrations to Form Thickness- and Modulus-Controlled SEI Layers on Lithium Metal Anodes. *J. Phys. Chem. C* **2018**, *122*, 9825–9834. [[CrossRef](#)]
34. Cheng, H.; Zhu, C.; Huang, B.; Lu, M.; Yang, Y. Synthesis and electrochemical characterization of PEO-based polymer electrolytes with room temperature ionic liquids. *Electrochim. Acta* **2007**, *52*, 5789–5794. [[CrossRef](#)]
35. Duan, H.; Yin, Y.X.; Zeng, X.X.; Li, J.Y.; Shi, J.L.; Shi, Y.; Wen, R.; Guo, Y.G.; Wan, L.J. In situ plasticized polymer electrolyte with double-network for flexible solid-state lithium-metal batteries. *Energy Storage Mater.* **2018**, *10*, 85–91. [[CrossRef](#)]

36. Hsu, S.T.; Tran, B.T.; Subramani, R.; Nguyen, H.T.T.; Rajamani, A.; Lee, M.Y.; Hou, S.S.; Lee, Y.L.; Teng, H. Free-standing polymer electrolyte for all-solid-state lithium batteries operated at room temperature. *J. Power Sources* **2020**, *449*, 227518. [[CrossRef](#)]
37. Vélez, J.F.; Aparicio, M.; Mosa, J. Covalent silica-PEO-LiTFSI hybrid solid electrolytes via sol-gel for Li-ion battery applications. *Electrochim. Acta* **2016**, *213*, 831–841. [[CrossRef](#)]
38. Popall, M.; Andrei, M.; Kappel, J.; Kron, J.; Olma, K.; Olsowski, B. ORMOCERs as inorganic-organic electrolytes for new solid state lithium batteries and supercapacitors. *Electrochim. Acta* **1998**, *43*, 1155–1161. [[CrossRef](#)]